ГОДИШНИК НА СОФИЙСКИЯ УНИВЕРСИТЕТ „СВ. КЛИМЕНТ ОХРИДСКИ"

ФАКУЛТЕТ ПО МАТЕМАТИКА И ИНФОРМАТИКА
Книга 2 — Механика
Том 81, 1987

ANNUAIRE DE L'UNIVERSITE DE SOFIA „ST. KLIMENT OHRIDSKI"

FACULTE DE MATHEMATIQUES ET INFORMATIQUE
Livre 2 — Mécanique
Tome 81, 1987

STOCHASTIC REGIME FOR KURAMOTO-SIVASHINSKY EQUATION PART II — NUMERICAL SIMULATION

BLAGOVEST SHARBANOV, CHRISTO I. CHRISTOV

Благовест Шарбанов, Христо И. Христов. СТОХАСТИЧЕСКИЙ РЕЖИМ ДЛЯ УРАВНЕНИЯ КУРАМОТО-СИВАШИНСКОГО. ЧАСТЬ II — ЧИСЛЕННЫЙ ЭКСПЕРИМЕНТ

Рассматривается эволюционное уравнение четвертого порядка по пространственной переменной (называемое некоторыми авторами уравнение Курамото–Сивашинского), которое дает слабонелинейное приближение для формы свободной поверхности стекающей вязкой пленки. Разработаны разностная схема и алгоритм численного решения и при их помощи детально исследован стохастический режим. Получены результаты для вторых и третьих кумулянтов (обобщенных корреляционых функций). Хорошее количественное совпадение с результатами первой части работы по аппроксимации решения точечной случайной функцией подтверждает эффективность этого подхода.

Blagovest Sharbanov, Christo I. Christov. STOCHASTIC REGIMÉ FOR KURAMOTO-SIVASHINSKY EQUATION. PART II — NUMERICAL SIMULATION

The fourth-order with respect to the spatial coordinate nonlinear equation of evolution (called by some authors Kuramoto–Sivashinsky equation) representing the weakly nonlinear approximation for the shape of free surface of falling thin viscous film is considered. A difference scheme and algorithm for numerical simulation of the solution are developed and by their means the stochastic regimé is thoroughly investigated and data is gathered for the second and third cumulants (generalized correlation functions). The good quantitative comparison with the results of the preceding part I of the paper speaks in the favour of the proposed there random point approximation.

As it is discussed in the preceding paper [1], the weakly nonlinear approxima-

tion for the thin viscous capillary film falling down a vertical plane yields for the shape of free surface a fourth–order equation of evolution called by some authors Kuramoto–Sivashinsky equation. Although its solution gives for the shape a fair qualitative prediction that compares well with the predictions of more complicated models (see, e. g. [2, 3]), the Kuramoto–Sivashinsky equation (hence–forth K–S equation) is not to be identified with the real flow in falling films and the experimental observations can not serve as a reliable basis for quantitative verification of different approximate models (e. g. the model of [1]) for the stochasticity of K–S equation. In this connection the K–S equation is akin to its famous counterparts Burgers and Korteweg – de Vries equation and, similarly to them, the only way to gather data about stochastic behaviour of the solution is to use a direct numerical simulation. For instance, for Burgers equation such a numerical experiment is performed in [4] and the results obtained there for the correlation function and spectrum prove decisive for assessment of the random point approximation proposed in [5] and developed further in [6]. The numerical simulation of Burgers equation is recently repeated and enlarged by the authors, monitoring also third- and fourth–order cumulants of the random solution, and will be published elsewhere. In the present paper a numerical algorithm is developed and the stochastic regimé of K-S equation is investigated compiling extensive data for the different averaged characteristics: moments, cumulants, spectra, etc.

1. STATEMENT OF THE PROBLEM AND DIFFERENCE SCHEME

Consider the K-S equation in the following dimensionless form

$$\frac{\partial \varphi}{\partial t} + \frac{3}{a}\frac{\partial \varphi}{\partial x} + 6\varphi\frac{\partial \varphi}{\partial x} + \frac{\partial^2 \varphi}{\partial x^2} + \frac{\partial^4 \varphi}{\partial x^4} = 0, \tag{1.1}$$

where a is the only governing parameter that is connected with the ratio of powers of Reynolds and Weber numbers.

Consider also a sufficiently large interval $x \in [-L, L]$ for the independent variable such that the influence of the boundary conditions on the solution near the origin of the coordinate system to be negligible. Provided that this interval is selected properly, the boundary conditions are not important and one can take the most covenient for the numerical scheme, namely

$$\varphi = 0, \quad \frac{\partial^2 \varphi}{\partial x^2} = 0 \quad \text{for} \quad x = \pm L. \tag{1.2}$$

Going a little bit ahead it can be said that the trivial solution of the boundary value problem (1.1)–(1.2) is not asymptotically stable (in the sense of Lyapunov), but it is not unstable either. As a result, the finite-amplitude disturbances develop and reach certain level which is not further exceeded. The resulted regimé is random. In order to shorten the required computational time for reaching the chaotic state we employ a random initial condition

$$\varphi_0(x, t_0) = C\beta_i \quad \text{for} \quad x \in [x_i, x_{i+1}), \tag{1.3}$$

where C is an arbitrary constant, $\{x_i\}$ is a set of regularly spaced points (the same grid is employed below in numerical computations) and β_i is a random variable that is a function of the index i and possesses Gausian probability distribution (Fig. 1). Here is to be mentioned that the initial condition is virtually delta-correlated with

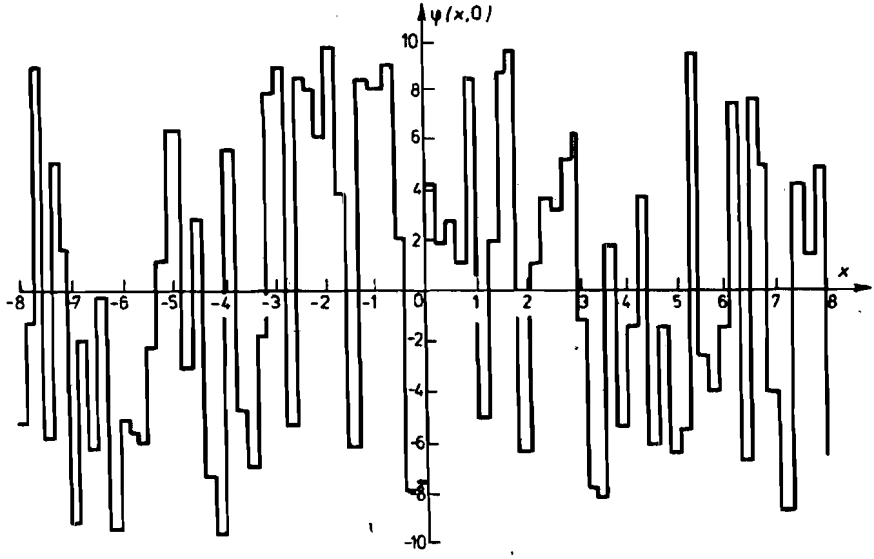

Fig. 1. The shape of the initial condition

respect to the spatial coordinate x (Fig. 2). Taking a sufficiently large value of C, we "inject" enough energy from the very beginning and it remains only to redistribute this energy according to the law expressed by (1.1).

The initial-boundary value problem (1.1)–(1.3) is solved numerically by means of difference scheme. As it has already been mentioned, the grid is assumed to be regularly spaced

$$x_i = -L + (i-1)h, \qquad h = 2L/(M-1), \tag{1.4}$$

where $2L$ is the total length of the interval and M is the number of grid points distributed over that interval. Respectively h is the spatial spacing. In the same manner is constructed the temporal mesh

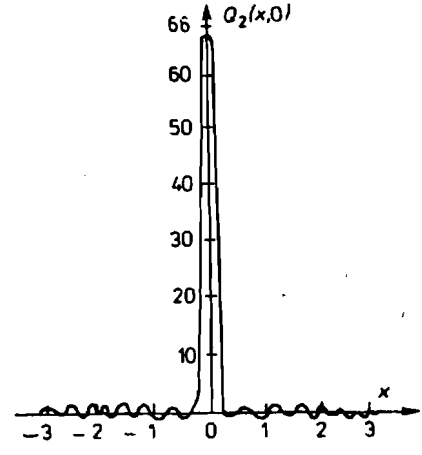

Fig. 2. The spatial correlation of the initial condition

$$t_j = t_0 + j\tau, \tag{1.5}$$

where t_0 is the initial moment of time and τ is the time increment.

The difference scheme employs second-order approximations for the first, second and fourth derivatives with respect to the spatial variable and a simple linearization. Denoting by φ_i^j the magnitude of the set function for $x = x_i$ and $t = t_j$ the difference scheme can be expressed as follows

$$(1.6)\qquad \frac{1}{h^4}\varphi_{i-2}^{j+1} + \left(-\frac{3}{2ah} - \frac{6\varphi_i^j}{2h} - \frac{4}{h^4} + \frac{1}{h^2}\right)\varphi_{i-1}^{j+1}$$
$$+ \left(\frac{1}{\tau} + \frac{6}{h^4} - \frac{2}{h^2}\right)\varphi_i^{j+1} + \left(\frac{3}{2ah} + \frac{6\varphi_i^j}{2h} - \frac{4}{h^4} + \frac{1}{h^2}\right)\varphi_{i+1}^{j+1}$$
$$+ \frac{1}{h^4}\varphi_{i+2}^{j+1} = \frac{1}{\tau}\varphi_i^j \quad \text{for} \quad i = 3, \ldots, M-2.$$

Obviously (1.6) is a five-diagonal linear algebraic system which is coupled by the difference approximations of the boundary conditions (1.2) taken at the points $i = 2$ and $i = M - 1$, namely,

$$(1.7)\qquad \begin{aligned} &\varphi_2 = 0, && \varphi_{M-1} = 0,\\ &\varphi_1 - 2\varphi_2 + \varphi_3 = 0, && \varphi_{M-2} - 2\varphi_{M-1} + \varphi_M = 0. \end{aligned}$$

The latter means that the "actual infinity" is taken at $\pm(L = h)$, which is not loosing the generality since the value L is at our disposal.

2. NUMERICAL EXPERIMENTS AND OPTIMAL VALUES OF PARAMETERS

For solving (1.6), (1.7), a special kind of Gaussian elimination method with pivoting is employed (see five-point "progonka" in [7]). It is to be noted here that for large M (and this is our case), the ordinary precision of about 10^{-7} is insufficient and the errors propagate, though the elimination method is theoretically stable. Only a double precision of about 10^{-16} secures stable elimination. In Fig. 3 is shown a typical realization of the random solution of K–S equation (for definiteness the initial moment of time is set equal to zero).

The most important question to be answered is connected with the quantities L, M and T. At the beginning a criterion is to be defined. As far as the purpose of the present work are the statistical characteristics, the most natural way is to consider one of these characteristics, say, the correlation function, as a criterion

$$(2.1)\qquad Q_2(x,t) = \frac{1}{2L_1}\int_{-L_1}^{L_1} \varphi(\xi,t)\varphi(\xi + x,t)\,d\xi - \overline{\varphi}^2,$$

where

$$(2.2)\qquad \overline{\varphi} = \frac{1}{2L_1}\int_{-L_1}^{L_1} \varphi(\xi,t)\,d\xi \cong \frac{1}{2L_1}\int_{-L_1}^{L_1} \varphi(\xi + x,t)\,d\xi$$

is the spatial average of φ which is virtually constant. Here $L_1 = 0.8L$ and respectively $x \in [-L_1, L_1]$.

Let us begin with the actual infinity L, which has to be kept large enough in order to exclude border effects, but is to be as small as possible to decrease the

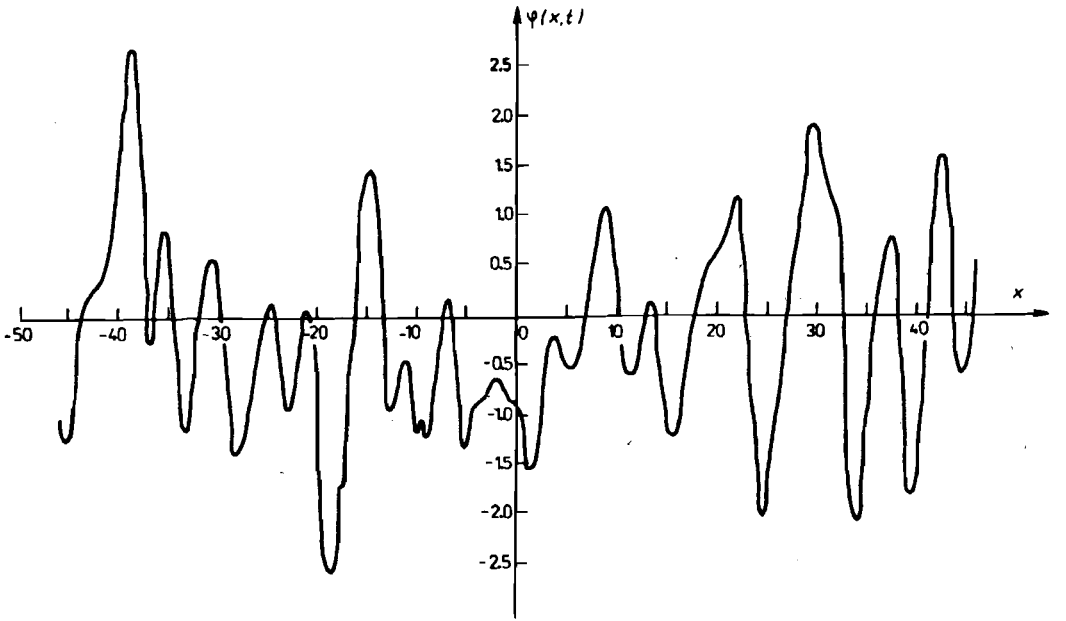

Fig. 3. A typical realization of the random solution to K–S equation with $a = 1$, $t = 1.2$, $h = 0.05$, $M = 12\,001$, $\tau = 0.01$

computational time. We increased stepwise L from 100 by increment of 10 and compared the results for Q_2. It turns out that $L = 300$ represents an optimum in the above described sense and difference in values of Q_2 with $L = 200$ and $L = 300$ is less than 1%, while the differences between 290 and 300 can not be discerned. So, the value $L = 300$ is chosen to represent the "infinity" and the rest of the computations are performed with that value.

The second (and perhaps the most important) problem is the optimal value for the spatial spacing h. It is to be small enough to secure acceptable approximation of the difference scheme, but not too small since the total number of grid points is $M = 1+2L/h$ (see (1.4)) and for very small h can soar intolerable high. Comparing once again the profile of the correlation function $Q_2(x,t)$ (see Fig. 4), we find that the spacings satisfying $h \leqq 0.1$ are acceptable. The main portion of the numerical results to follow are obtained with $h = 0.5$ which gives $M = 12\,001$ under the adopted value of L. This number of points is at the upper extreme of the capabilities of the available computer.

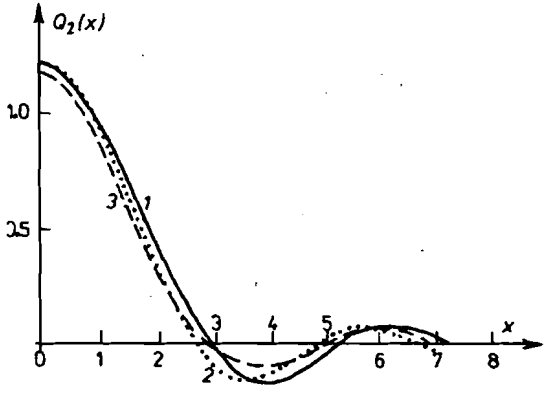

Fig. 4. Dependence of the correlation function Q_2 on the spacing h for $a = 1$ and $t = 1$: *1* — $h = 0.2$; *2* — $h = 0.1$; *3* — $h = 0.05$

The third problem to tackle is the value $t = T$ for which the results are to be taken. This value must be large enough to allow the solution to "forget" the initial conditions and must be kept as small as possible in order to lower the amount of used computational time. In Fig. 5 are depicted the respective results. It is seen that $T = 1$ is good enough to obtain solution which is statistically converged to the steady-state stochastic solution (solution for which all statistical characteristics are not functions of time while the solution inself is a function of time).

3. RESULTS AND COMPARISONS

The main statistical characteristics of a random function are the multi-point correlation functions (cumulants) and the relative multi-spectra. Naturally, the first to undergo investigation is the correlation function (2.1). In this section it is calculated for different values of the only governing parameter a and compared

to the predictions of the random point approximations of [1]. These results are depicted in Fig. 6. One sees that the results for $a = 0.8$ compare very well with those predicted from Poisson random train of solitions with $c = 5$. In this case for the dimensionless phase velocity (celerity) one obtains $V = 8.75$. Respectively, the case $a = 1.333$ is modelled adequately by Poisson ensemble of solitons with parameter $c = 1$, which gives $V = 3.25$. As elucidated in [1] the mere Poisson random function is a rather rough approximation, but in many situations it is fully capable of good quantitative prediction for the mean values and for the correlation function when moderate correlation distances are considered. This effect is observed in the present results

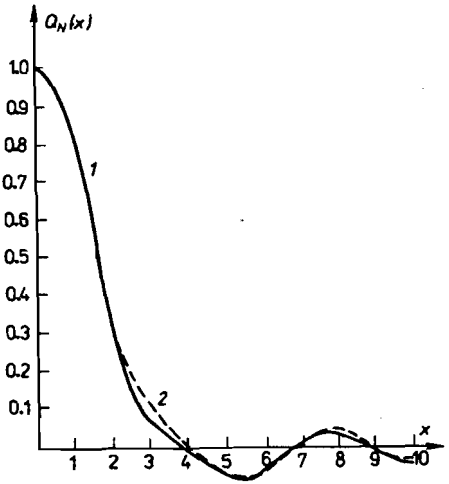

Fig. 5. Developing the correlation function Q_2 with the time t for $a = 1$, $h = 0.05$, $L = 300$: *1* — $t = 1.2$; *2* — $t = 2.4$

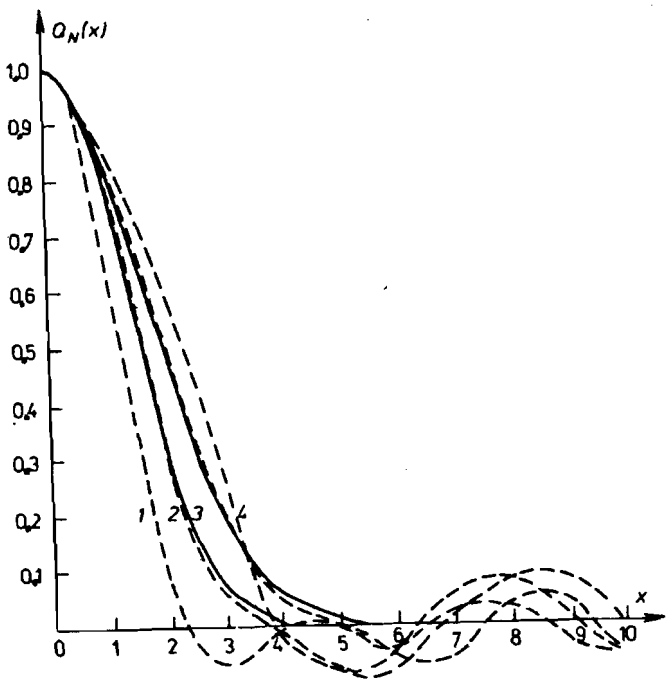

Fig. 6. The normalized correlation function Q_N for $h = 0.05$, $L = 300$ and different a (dashed lines): *1* — $a = 0.6$; *2* — $a = 0.8$; *3* — $a = 1.33$; *4* — $a = 1.666$ versus prediction of the random point approximations with different c (continuous lines): *2* — $c = 5$; *3* — $c = 1$

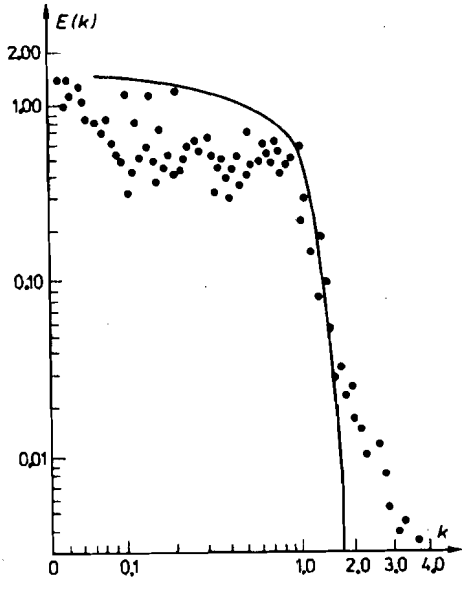

Fig. 7. The spectrum of the simulated solution (points) for $h = 0.05$, $L = 300$, $a = 1.333$ and comparison with the prediction of the random point approximation (line) for $c = 1$

too. The good quantitative agreement means that for $a = 0.8$ the solitons with phase velocities $V = 8.75$ prevail in the random train. Respectively, for $a = 1.333$ — so do the solitons with $V = 3.25$.

An interesting discrepancy shows up in Fig. 6. That is the nonmonotonic behaviour of the experimental correlation versus monotonic one of the predicted correlation. This observation is very similar to situation for Lorenz attractor [8], where it is attributed to the two-point probability density, significantly deviating from the Poisson case. We believe that the same reason is responsible for the discrepancy in our case too. Still, deviation are for large correlation distances and the Poisson approximation is not compromised as far as the moderate correlation distances are considered.

From the correlation function Q_2 it can be calculated the spectrum

$$E(k,t) = \int_{-\infty}^{\infty} Q_2(x,t)\cos(2\pi kx)\,dx, \tag{3.1}$$

where k is the wave number. The infinite bounds are replaced by L. The latter is done to exclude the adjacent to boundaries points where the influence of the more or less artificial boundary condition can prove significant. The numerical scheme for (3.1) is based on the notion of fast Fourier transformation, namely

$$E(k_j,T) = 2\sum_{i=1}^{M_1}\left\{\left[\frac{1}{2\pi k_j}(Q_{i+1}\sin k_j x_{i+1}2\pi - Q_i \sin 2\pi k_j x_i) + \frac{Q_{i+1}-Q_i}{x_{i+1}-x_i}\frac{(2\pi)^{-2}}{k_j^2}(\cos 2\pi k_j x_{i+1} - \cos k_j x_i)\right](x_{i+1}-x_i)\right\}, \tag{3.2}$$

where it is acknowledged that the correlation function is even one and, hence, the spectrum has only real part. The number of points $M_1 = L_1/h+1$ and $x_i = (i-1)h$.

In Fig. 7 the experimental data are shown for the spectrum obtained with $a = 1.333$ and compared with the prediction of the Poisson random point function with $V = 3.25$ (the same situation as curve 3 in Fig. 6). It is interesting to note that the asymptotic behaviour of the spectrum differs significantly for large k. In our oppinion this is connected with the discretization in numerical experiment and with the size of the spacing h. If one is bound to represent adequately the high-frequence motion ($k \gg 1$), a very small h is to be adopted which is not possible on the available computer.

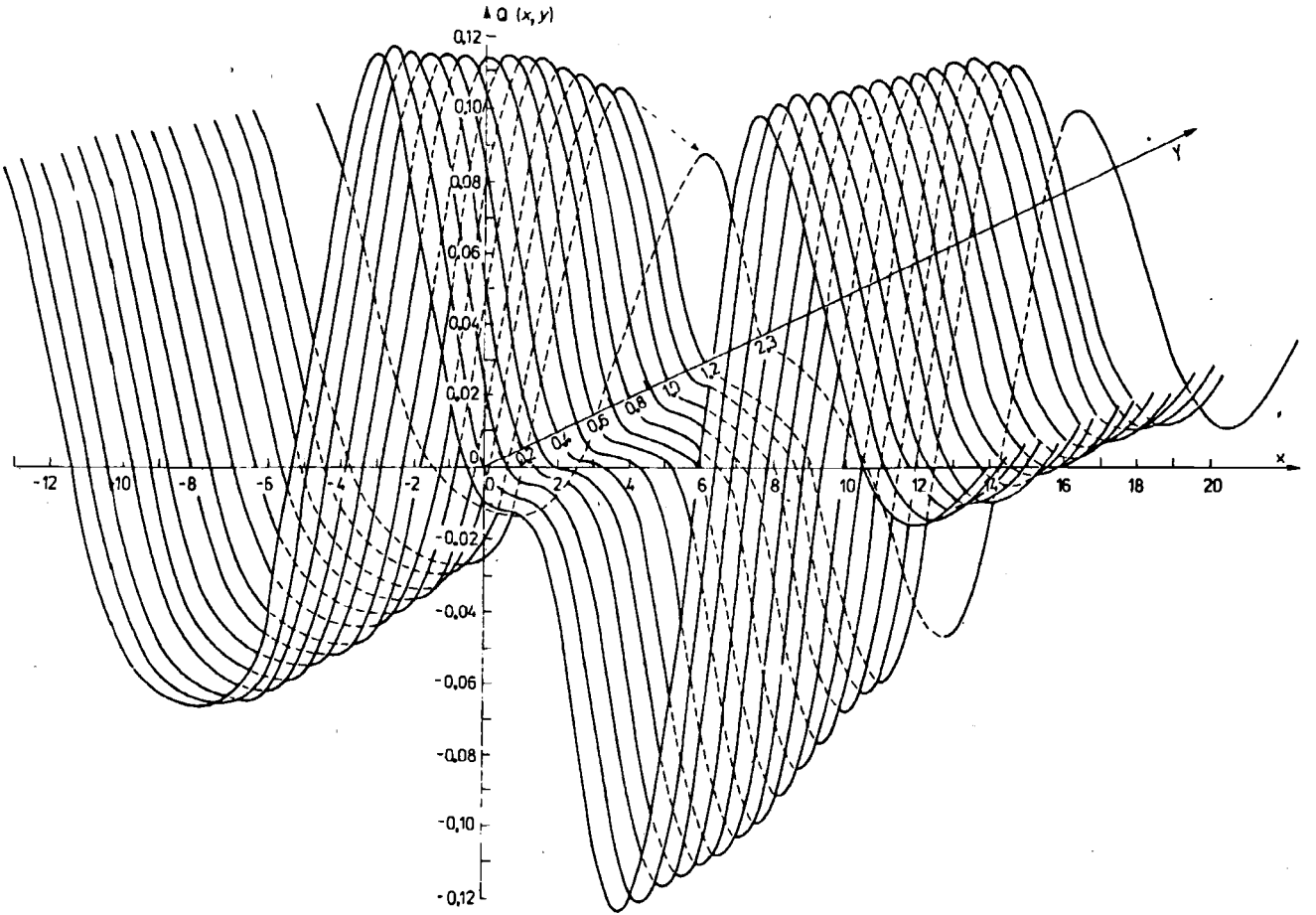

Fig. 8. The surface of the three-point correlation function $Q_3(x, y)$ for $h = 0.05$, $L = 300$, $L_1 = 240$, $a = 1.333$

In the end we compute the third-order cumulant (generalized correlation function):

$$Q_3(x,y,t) = \frac{1}{2L_1}\int_{-L_1}^{L_1} \varphi(\xi,t)\varphi(\xi+x,t)\varphi(x+y,t)\,d\xi - [Q_2(x,t)+Q_2(y,t)+Q_2(y-x,t)]\overline{\varphi} - \overline{\varphi}^3. \tag{3.3}$$

The results are presented in Fig. 8. Due to the obvious symmetry, leaving Q_3 invariant when interchanging x and y, we choose different scales for x and y in order to make the figure more informative. Naturally, the function Q_3 decays to zero for $y \to \infty$ or $x \to \infty$, but rather slowly, exhibiting a number of local minima and maxima. In this instance it resembles the correlation function for the third unknown in Lorenz attractor and is a result of the intricate shape of the two-point probability density of the system of generating random points. The result for the third cumulant shall be very useful when the model of [1] is generalized to incorporate the said probability densities.

CONCLUDING REMARKS

The results of the present paper show that the stochastic regimé for Kuramoto–Sivashinsky equation can be investigated numerically by means of difference scheme. The second conclusion is that the approximation with Poisson random point function is fully adequate for moderate correlation distances.

LITERATURE

1. Christov, C. I. Stochastic regimé for Kuramoto-Sivashinsky equation, Part I — Random point approximation. — Ann. Univ. Sofia, Fac. Math. Inf., **81**, 1987, livre 2 — Mécanique, this volume.
2. Pumir, A., P. Manneville, Y. Pomeau. On solitary waves running down an inclined plane. — J. Fluid Mech., **135**, 1983, 27–50.
3. Бубнов, А. В., Е. А. Демехин, В. Я. Шкадов. Бифуркации уединенных волн в стекающем слое жидкости. — Изв. Моск. Университета, сер. 1. Мат. и мех., 1986, № 2, 73–78.
4. Jeng, D. T., R. Forester, S. Haaland, W. Meecham. Statistical initial-value problem for Burgers model equation of turbulence. — Phys. Fluids, **9**, 1966, 2114–2120.
5. Христов, Х. И. Об одном каноническом разложении случайных процессов и его применение к турбулентности. — БАН ТПМ, **11**, 1980, № 1, 59–66.
6. Christov, C. I. Poisson–Wiener expansion in nonlinear stochastic systems. — Ann. Univ. Sofia, Fac. Math. Mech., **75**, 1981, 1985, livre 2 — Mécanique, 143–165.
7. Самарский, А. А., Е. Н. Николаев. Методы решения сеточных уравнений, Наука, М., 1978.
8. Christov, C. I. The method of random point approximation for nonlinear stochastic system — application to Lorenz attractor. — Comp. Rend. Acad. Bulg. Sci., **41**, 1988.

Received 4.01.1988